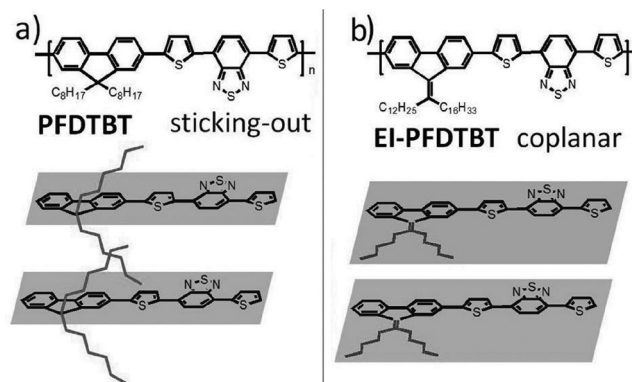COMMUNICATION

Highly Crystalline and Low Bandgap Donor Polymers for Efficient Polymer Solar Cells

Jun Liu, Hyosung Choi, Jin Young Kim, Chris Bailey, Michael Durstock, and Liming Dai*

Polymer solar cells (PSCs) have recently attracted great attention because of their potential advantages, including flexibility, light weight, and low fabrication cost.[1–4] Photon absorption by conjugated polymers often creates bound electron/hole pairs (i.e., excitons). Charge collection, therefore, requires dissociation of the excitons, a process which is known to be favorable at the interface between conjugated polymers as donors and C_{60} derivatives as acceptors. Since [6,6]-phenyl-C_{61}-butyric acid ester (PCBM) is still one of the best electron acceptors, most recent efforts have focused on the development of low bandgap donor polymers.[5–22] Examples of low bandgap polymers include conjugated polymers having electron-donating (D) and electron-accepting (A) moieties in the main chain.[21,22] The bandgap of the D-π-A polymers can be effectively reduced through intramolecular charge transfer while their physical properties can be readily tuned by tailoring structures of the D and A moieties and/or the linking bridge. An ideal donor polymer should have a broad absorption spectrum for an efficient solar photon harvesting, a low HOMO level for a high open-circuit voltage (V_{OC}), a good compatibility with PCBM for the formation of a bi-continuous network (i.e., bulk heterojunction, BHJ) with a large interface area, and a high hole mobility for an efficient transportation of the photo-generated charge carriers.[4] When designing donor polymers, therefore, a delicate balance between the crystallinity and the solubility needs to be taken into consideration.[5] Highly crystalline conjugated polymers with closely packed polymer chains in the solid state often show high hole mobility, but low solubility in organic solvents. Although the high hole mobility is an asset to PSCs, highly crystalline polymers with poor solution-processability rarely form the desired bi-continuous morphology with PCBM, and hence usually exhibit poor photovoltaic performance. In the present study, we have devised a general approach to D-π-A polymers that not only have a low bandgap but also a high crystallinity

using ethylene bridging units to ensure a coplanar configuration between the polymer backbone and the side chains. Based on the above discussion, the resultant highly crystalline and low bandgap polymers should be highly desirable donors for high-performance BHJ PSCs. In view of the poor processability associated with most highly crystalline polymers, we have also developed a new method for the PSC device construction by solution-casting the newly synthesized highly crystalline polymers at an elevated temperature (120 °C).

Side chains of a donor polymer play an important role in controlling the polymer crystallinity by regulating the stacking of the main chain.[23,24] In most of the reported D-π-A donor polymers, the side chains are bonded to the sp^3 hybridized C or Si bridging atom along the polymer backbone.[8–22,25] Owing to the sp^3 hybridization of the bridging atoms, the side chains "stick out" from the main chain plane and impede a close packing of the main chains.[8–22] **Figure 1** shows chemical structures for the D-π-A donor polymer synthesized in this study (Figure 1b) and its analogues reported in the literature,[10,11,13] which can be used for discussion on the bridging unit effect. Although PFDTBT (Figure 1a) has two alkyl side chains connected to the C atom with a "sticking-out" configuration to prevent close packing of the main chains, this amorphous polymer is still an efficient donor because of its relatively low bandgap.[10,11] By inserting an ethylene bridging unit between the side chain and the main chain of the D-π-A donor polymer synthesized in this study (i.e., EI-PFDTBT, Figure 1b), we can effectively eliminate the undesired steric hindrance effect of the side chains. Because of the sp^2 hybridization of the carbon atoms in the ethylene unit, the side chains and the main chain in EI-PFDTBT adopt a coplanar configuration, as schematically shown in

Dr. J. Liu, Prof. L. Dai
Department of Macromolecular Science and Engineering
Case School of Engineering
Case Western Reserve University
10900 Euclid Avenue, Cleveland, OH 44106, USA
E-mail: liming.dai@case.edu
H. Choi, Prof. J. Y. Kim
Interdisciplinary School of Green Energy
Ulsan National Institute of Science and Technology (UNIST)
Ulsan 689-798, Republic of Korea
Dr. C. Bailey, Dr. M. Durstock
Materials and Manufacturing Directorate
Air Force Research Laboratory
RXBP, Wright-Patterson Air Force Base, OH 45433, USA

Figure 1. Schematic illustration of the side chain configuration of PFDTBT (a) and EI-PFDTBT (b). For clarity, all the alkyl side chains, including one branched and long alkyl chain, are simplified. The chemical structures of the two polymers are also shown.

Figure 1b. This coplanar configuration could facilitate a close intermolecular π–π stacking between the main chains, leading to a high hole mobility for efficient PSCs. To the best of our knowledge, there has been no reported work on the use of an ethylene bridging unit in donor polymers for the formation of a coplanar configuration between the side chains and the conjugated main chain when this project was initiated.[25]

A literature survey shows that crystal structures of two model molecules, 2,7-dibromo-9,9-dioctylfluorene (Figure S1a, Supporting Information)[26] and 2,7-dibromo-9-(1′-hexylheptylidene)fluorene (Figure S1b),[27] have been reported. It was found that the two octyl chains directly connected to the sp^3 hybridized C atom at the 9 position of fluorene in Figure S1a are perpendicular to the fluorene plane whereas the hexyl chains in Figure S1b are coplanar with the fluorene unit because of the sp^2 hybridized C in the ethylene unit. Consequently, the ethylene bridging unit can be used to improve crystallinity for polymers with side chins bonded to the main chain through an sp^3 hybridized C or Si atom.[10–20] On this basis, we have devised EI-PFDTBT with a bridging ethylene unit between the flanking side chains and the main chain (Figure 1b), which is expected to show significantly improved photovoltaic performance over the existing efficient donor polymer PFDTBT. In spite of the above-mentioned processing difficulties associated with highly crystalline polymers, we have achieved a power conversion efficiency (PCE) exceeding 5% by spin-coating the EI-PFDTBT/PC$_{71}$BM blend solution at an elevated temperature (120 °C) in this study.

Scheme 1 shows the synthetic route for EI-PFDTBT while detailed experimental procedures and structural characterization can be found in the Supporting Information. The key monomer **4** was readily synthesized by a four-step reaction, followed by copolymerization with commercially available monomer **5** to afford EI-PFDTBT. The chemical structure of EI-PFDTBT was verified by ^{1}H NMR and elemental analyses (see Supporting Information). The viscosity-average molecular weight was determined by a Ubbelohde viscometer to be 45 000 (GPC measurements were tried without success). The resultant EI-PFDTBT exhibits a good thermal stability with a decomposition temperature (T_d) of 385 °C, as revealed by thermogravimetric analyses (TGA, Figure S2, Supporting Information). The HOMO and LUMO levels of EI-PFDTBT were calculated, from the onset potentials of the oxidation and reduction peaks in the cyclic voltammogram (Figure S3, Supporting Information), to be –5.31 and –3.61 eV, respectively. The deep-lying HOMO level of EI-PFDTBT suggests a high V_{oc} for the PSC devices to be developed (see below).[28] The energy levels of EI-PFDTBT are very close to those of
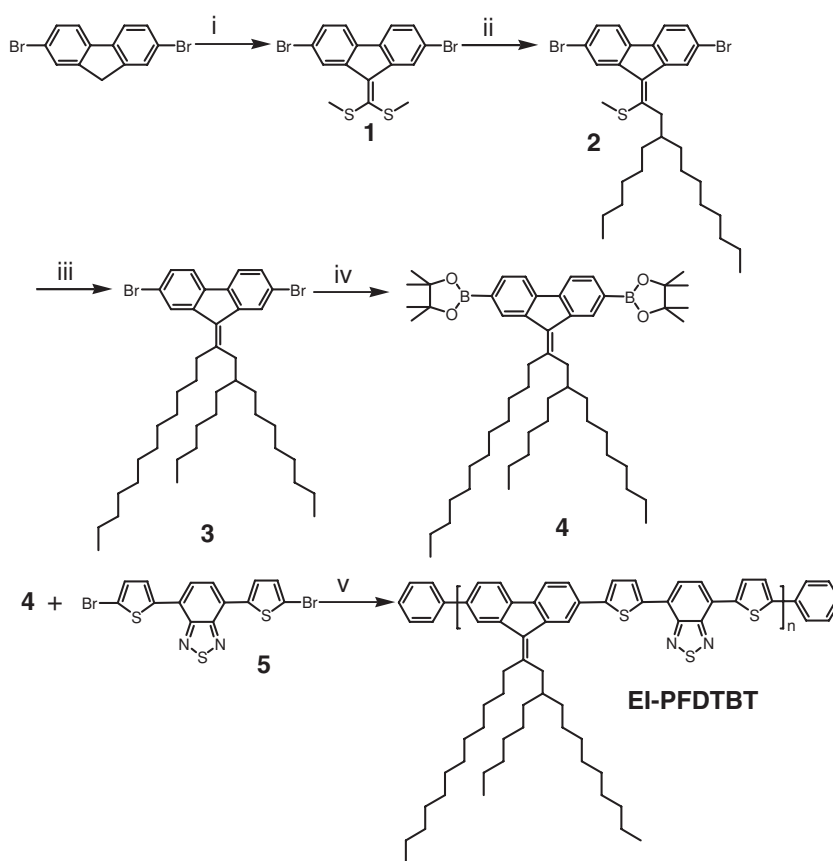
Scheme 1. Synthetic route to the EI-PFDTBT polymer (reagents and conditions: i) NaOC$_4$H$_9$, CS$_2$, CH$_3$I, DMSO, r.t.; ii) Li$_2$CuCl$_4$, C$_{16}$H$_{33}$MgBr, THF; iii) Li$_2$CuCl$_4$, n-C$_{12}$H$_{25}$MgBr, THF; iv) Pd(dppf)$_2$Cl$_2$, KOAc, bis(pinacolato)diboron, 1,4-dioxane, 80 °C; v) Pd (PPh$_3$)$_4$, toluene, 1,4-dioxane, tetrabutylammonium hydroxide, 90 °C).

the analogous polymer PFDTBT,[10–13] indicating a negligible effect of the ethylene bridging unit on the bandgap structure of the polymer main chain. As expected, however, the insertion of the ethylene unit caused a significant effect on the π–π packing of the main chains in EI-PFDTBT, as confirmed by X-ray diffraction (XRD) and UV/Vis absorption spectroscopic measurements.

Figure 2a reproduces the XRD profile for a EI-PFDTBT powder. The strong diffraction peak at 21.3° indicates the 4.1 Å π-stacking spacing between polymer layers along the z-direction while the peak at 3.9° corresponding to 22.6 Å is attributable to the spacing between the polymer main chains separated by the side chains in the plane. Figure 2b shows UV-Vis absorption spectra for EI-PFDTBT in dichlorobenzene (10^{-5} M) and in the solid state. As can be seen, the absorption maximum red-shifted from 550 nm for the solution at 150 °C to 601 nm in the solid film. The observed 51 nm red-shift clearly indicates that a close π–π stacking in the solid state has been achieved for EI-PFDTBT with a coplanar configuration between the side chains and main chain. The absorption spectrum of EI-PFDTBT at 25 °C also shows a significant red-shift compared with that at 150 °C because of the strong
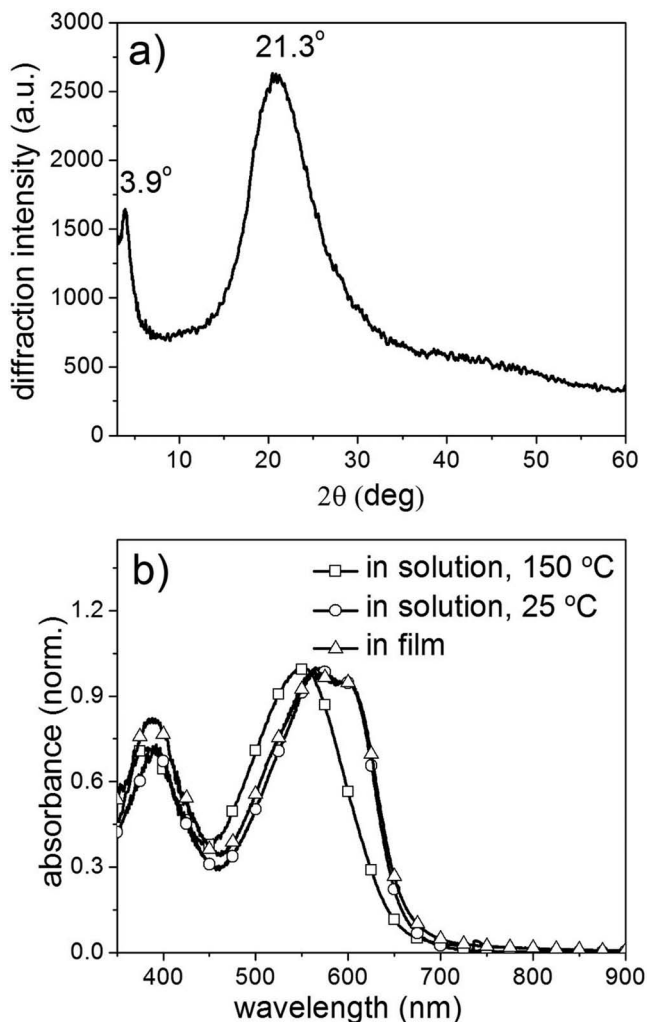
Figure 2. a) X-ray diffraction pattern of EI-PFDTBT powder. b) UV-Vis absorption spectra of EI-PFDTBT in *o*-dichlorobenzene solution and in solid film.

π–π stacking of the main chain at the low temperature even in solution. In contrast, PFDTBT having a non-coplanar configuration with two "sticking out" side chains per monomer unit is amorphous without any XRD peak.[10] PFDTBT also shows a small red-shift (5 nm) in the absorption peak from solution to the solid state,[10] indicating a disordered film structure because of the weak interchain interaction of the PFDTBT main chains with large steric hindrance induced by the "sticking out" alkyl side chains (see Figure 1a). The close π–π packing seen in the EI-PFDTBT film (Figures 1b and 2a) could greatly facilitate charge carrier hopping along the polymer main chains to enhance the charge carrier mobility in PSCs. Furthermore, the large red-shift associated with the optical absorption peak of the EI-PFDTBT film indicates a much improved solar absorption capability. Both the enhanced hole mobility and solar absorption capability could improve the photovoltaic performance of EI-PFDTBT.

The photovoltaic properties of EI-PFDTBT were investigated with the device structure of ITO/PEDOT:PSS/

EI-PFDTBT:PC$_{71}$BM(1:2)/Ca/Al (ITO, indium tin oxide; PEDOT:PSS, poly(styrene sulfonate) doped poly(ethylenedioxy-thiophene). The current density–voltage (*J*–*V*) curves of the devices under simulated AM1.5G illumination are shown in **Figure 3**a while the characteristics of the devices are listed in **Table 1**. As can be seen in Figure 3a, the PSC device with the active layer spincoated at room temperature (20–25 °C) exhibits a poor performance with a PCE of only 1.53%. Conventional device optimization approaches, including thermal annealing, solvent annealing, solvent optimization, and solvent additive, have been applied, all leading to a decreased PCE (see the Supporting Information). However, the device performance is greatly improved by spincoating the polymer active layer at elevated temperatures. In fact, the device constructed by spincoating the polymer active layer at 120 °C exhibits a V_{OC} of 0.85 V, short-circuit current density (J_{SC}) of 11.04 mA cm^{-2}, and fill factor (FF) of 0.54, leading to a PCE of 5.07%. This value of PCE is among the highest reported for PSCs based on similar low-bandgap polymers. Figure 3b shows the external quantum efficiency (EQE) spectra of the devices. For the device with spincoating at 120 °C, the maximum EQE is 64%, indicating efficient photon-to-electron conversion. The relatively low FF value suggests that there is still considerable room for further improvement in the device performance through careful optimization of the spincoating conditions, the morphology of the active layer, and the device structure.

The greatly enhanced photovoltaic efficiency by high temperature solution processing can be attributed to the thermally induced self-ordering of the chain into the desirable bi-continuous morphology with a relatively high crystallinity in the active layer. Figure 3c–e show atomic force microscopy (AFM) images of the active layer spincoated at 25, 80, and 120 °C, respectively. The corresponding photographs are given in Figure S4a–c, Supporting Information. As shown in Figure 3c and S4a, the active layer spincoated at 25 °C exhibits a very rough surface with plenty of large particles. In contrast, the uniform and smooth film formed at 120 °C is pinhole-free and particle-free (Figure 3e and S4c). The root mean square (rms) roughnesses for the films spincoated at 25, 80, and 120 °C are 5.79, 4.70, and 1.79 nm, respectively. The observed smooth surface indicates a good miscibility between EI-PFDTBT and PC$_{71}$BM without strong phase separation, leading to an improved device performance. These results reveal great potential for the high temperature processing to be used for constructing high-performance PSCs from highly crystalline polymers.

In conclusion, we have developed a new class of highly crystalline, low bandgap D-π-A polymers using ethylene bridging units to ensure a coplanar configuration between the side chains and main chain. High efficiency polymer solar cells with a power conversion efficiency exceeding 5% have been constructed from the newly-synthesized polymer by solution-processing at elevated temperatures. Using the elevated-temperature solution processing demonstrated in this study, therefore, high-performance PSCs could be constructed from many (semi-)crystalline polymers previously reported to be insoluble and incompatible with PCBM for photovoltaic applications.

Materials
Views
www.MaterialsViews.com

ADVANCED
MATERIALS
www.advmat.de

COMMUNICATION
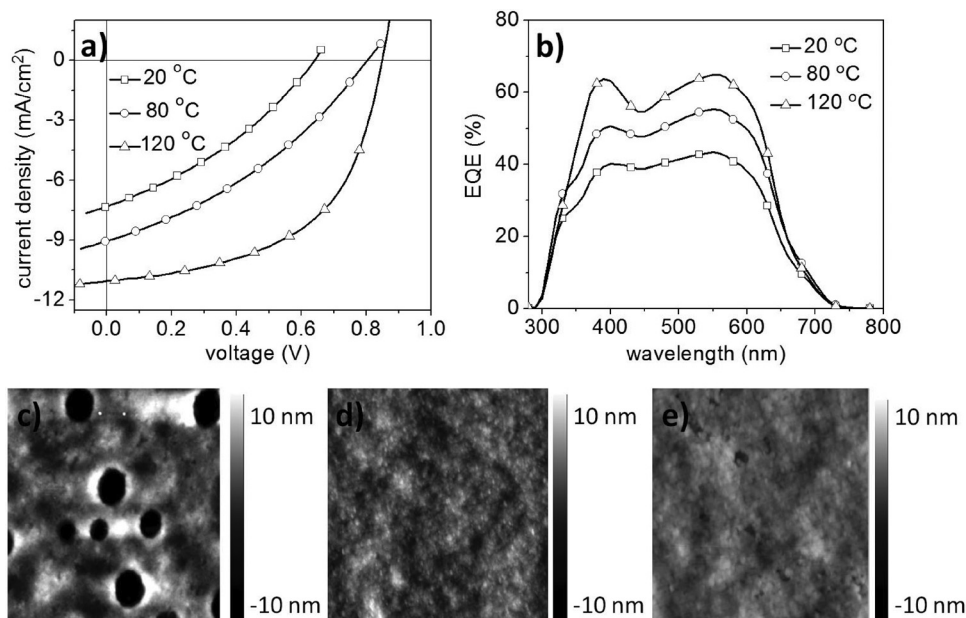
Figure 3. J–V curves (a) and EQE spectra (b) under AM1.5G irradiation of the devices based on EI-PFDTBT:PC$_{71}$BM = 1:2 with the active layers spincoated at specific temperatures. AFM images (3 μm × 3 μm) of EI-PFDTBT:PC$_{71}$BM = 1:2 films spincoated from 1,2,3-trichlorobenzene solution at 25 (c), 80 (d), and 120 °C (e).

Table 1. Characteristics of devices based on a EI-PFDTBT:PC$_{71}$BM active layer spincoated at different temperatures.

Temperature [°C]	V_{OC} [V]	J_{SC} [mA cm^{-2}]	FF	PCE [%]
25	0.64	7.31	0.34	1.59
80	0.80	9.02	0.35	2.52
120	0.85	11.04	0.54	5.07

Experimental Section

Synthesis of EI-PFDTBT: A mixture of 2,7-di(4,4,5,5-tetramethyl-1,3,2-dioxaborolan-2-yl)-9-(9-hexyltricosan-11-ylidene)-9H-fluorene (**4**) (0.247 g, 0.300 mmol), 4,7-bis(5-bromothiophen-2-yl)benzo[c][1,2,5]thiadiazole (**5**) (0.137 g, 0.300 mmol), Pd(PPh$_3$)$_4$ (0.006 g, 0.006 mmol), toluene (5 mL), 1,4-dioxane (1.5 mL), and 20% aqueous tetrabutylammonium hydroxide (1.5 mL) was degassed and stirred at 90 °C for 6 h in the dark. Phenylboronic acid 1,3-propanediol ester was then added and the mixture was stirred for another 2 h. Bromobenzene was added and the resulting mixture was stirred for 2 h. After cooling to room temperature, the mixture was poured into methanol and the precipitate was collected and washed with water. The precipitate was purified by Soxhlet extraction sequentially with acetone, hexane, chloroform, and chlorobenzene for 24 h each. The chlorobenzene fraction was collected and concentrated, followed by pouring into methanol. The dark solid was collected and dried under vacuum. Yield: 0.122 g (46.7%). ^{1}H NMR (600 MHz, d^4-*o*-dichlorobenzene, δ): 8.17 (br, 2H), 7.68 (br, 8H), 7.43 (br, 2H), 3.31 (br 4H), 2.18 (br, 1H), 1.90-1.00 (br, 44H), 0.76 (br, 9H). Anal Calcd. for C$_{57}$H$_{72}$N$_2$S$_3$: C 77.67, H 8.23, N 3.18. Found: C 77.41, H 8.58, N 2.87.

PSC Device Fabrication and Characterization: Patterned ITO glass substrates (sheet resistivity: 15 Ω per square) were ultrasonicated sequentially in detergent, deionized water, acetone, and iso-propyl alcohol for 10 min each. The substrates were dried with N$_2$ flow and then subjected to UV-ozone treatment for 15 min. A solution of PEDOT:PSS (Clevios VP Al 4083 from H. C. Starck Inc.) was spincoated onto the cleaned ITO substrate at 5000 rpm for 40 s and then baked at 140 °C for 10 min to give a thickness of 30 nm. The active layer was then spincoated on the PEDOT:PSS layer from the solution of EI-PFDTBT:PC$_{71}$BM = 1:2 in 1,2,4-trichlorobenzene (EI-PFDTBT concentration: 10 mg mL^{-1}) at 1000 rpm for 60 s. For devices undergoing high temperature processing, both the solution and the ITO/PEDOT:PSS glass substrate were heated on a hotplate at a specific temperature and then used for spincoating immediately. The spin-coated sample was then heated at 70 °C for 10 min, followed by transferring to a vacuum chamber. Finally, a 30 nm film of Ca and a 100 nm film of Al were sequentially deposited by thermal evaporation at 10^{-7} torr. The area of each device was 0.10 cm^2. The current density–voltage (J–V) curves of the devices were obtained using a Keithley 2400 source meter and a Newport Oriel sol 2A solar simulator (AM1.5G, 300 W). The light intensity was calibrated to be 100 mW cm^{-2} using a calibrated Si solar cell, which had been standardized by the National Renewable Energy Laboratory.

Supporting Information

Supporting Information is available from the Wiley Online Library or from the author.

Acknowledgements

[1] G. Yu, J. Gao, J. C. Hummelen, F. Wudl, A. J. Heeger, *Science* **1995**, *270*, 1789.

[2] B. C. Thompson, J. M. J. Fréchet, *Angew. Chem. Int. Ed.* **2008**, *47*, 58.

[3] G. Li, V. Shrotriya, J. S. Huang, Y. Yao, T. Moriaty, K. Emery, Y. Yang, *Nat. Mater.* **2005**, *4*, 864.

[4] G. Dennler, M. C. Scharber, C. J. Brabec, *Adv. Mater.* **2009**, *21*, 1323.

[5] F. He, W. Wang, W. Chen, T. Xu, S. B. Darling, J. Strzalka, Y. Liu, L. P. Yu, *J. Am. Chem. Soc.* **2011**, *133*, 3284.

[6] H.-Y. Chen, J. H. Hou, S. Q. Zhang, Y. Y. Liang, G. W. Yang, Y. Yang, L. P. Yu, Y. Wu, G. Li, *Nat. Photon.* **2009**, *3*, 649.

[7] Y. Y. Liang, L. P. Yu, *Acc. Chem. Soc.* **2010**, *43*, 1227.

[8] H. Zhou, L. Yang, S. C. Price, K. J. Knight, W. You, *Angew. Chem. Int. Ed.* **2010**, *43*, 4609.

[9] M. M. Wienk, M. Turbiez, J. Gilot, R. A. J. Janssen, *Adv. Mater.* **2008**, *20*, 2556.

[10] M. Svensson, F. Zhang, S. C. Veenstra, W. J. H. Verhees, J. C. Hummelen, J. M. Kroon, O. Inganäs, M. R. Andersson, *Adv. Mater.* **2003**, *15*, 988.

[11] M. H. Chen, J. H. Hou, Z. R. Hong, G. W. Yang, S. Sista, L.-M. Chen, Y. Yang, *Adv. Mater.* **2009**, *21*, 4238.

[12] E. G. Wang, L. Wang, L. F. Lan, C. Luo, W. L. Zhuang, J. B. Peng, Y. Cao, *Appl. Phys. Lett.* **2008**, *92*, 033307.

[13] N. Blouin, A. Michaud, M. Leclerc, *Adv. Mater.* **2007**, *19*, 2295.

[14] Z. G. Zhu, D. Waller, R. Gaudiana, M. Morana, D. Mühlbacher, M. Scharber, C. Brabec, *Macromolecules* **2007**, *40*, 1981.

[15] J. H. Hou, H. Y. Chen, S. Q. Zhang, G. Li, Y. Yang, *J. Am. Chem. Soc.* **2008**, *130*, 16144.

[16] J.-Y. Wang, S. K. Hau, H.-L. Yip, J. A. Davies, K.-S. Chen, Y. Zhang, Y. Sun, A. K.-Y. Jen, *Chem. Mater.* **2011**, *23*, 765.

[17] C. P. Chen, S. H. Chan, T. C. Chao, C. Ting, B. T. Ko, *J. Am Chem. Soc.* **2008**, *130*, 12828.

[18] L. Liao, L. M. Dai, A. Smith, M. Durstock, J. P. Lu, J. F. Ding, Y. Tao, *Macromolecules* **2007**, *40*, 9406.

[19] H.-Y. Chen, J. Hou, A. E. Hayden, H. Yang, K. N. Houk, Y. Yang, *Adv. Mater.* **2010**, *22*, 371.

[20] M. C. Scharber, M. Koppe, J. Gao, F. Cordella, M. A. Loi, P. Denk, M. Morana, H.-J. Egelhaaf, K. Forberich, G. Dennler, R. Gaudiana, D. Waller, Z. Zhu, X. Shi, C. J. Brabec, *Adv. Mater.* **2010**, *22*, 367.

[21] Q. Peng, K. Park, T. Lin, M. Durstock, L. Dai, *J. Phys. Chem. B* **2008**, *112*, 2801.

[22] Q. Peng, X. J. Liu, D. Su, G. W. Fu, J. Xu, L. Dai, *Adv. Mater.* **2011**, *23*, 4554.

[23] L. Q. Yang, H. X. Zhou, W. You, *J. Phys. Chem. C* **2010**, *114*, 16793.

[24] H. Bronstein, D. S. Leem, R. Hamilton, P. Woebkenberg, S. King, W. Zhang, R. S. Ashraf, M. Heeney, T. D. Anthopoulos, J. de Mello, I. McCulloch, *Macromolecules* **2011**, *44*, 6649.

[25] a) Our initial results were described at the AFOSR-ONR photovoltaic cell project review meeting in DC on June 28, 2011; b) C. Du, C. Li, W. Li, X. Chen, Z. Bo, C. Veit, Z. Ma, U. Wuerfel, H. Zhu, W. Hu, F. Zhang, *Macromolecules* **2011**, *44*, 7617.

[26] M. Leclerc, M. Ranger, F. Belanger-Garipy, *Acta Crystallogr.* **1998**, *C54*, 799.

[27] M. Heeney, C. Bailey, M. Giles, M. Shkunov, D. Sparrowe, S. Tierney, W. Zhang, I. McCullough, *Macromolecules* **2004**, *37*, 5250.

[28] M. C. Scharber, D. Muhlbacher, M. Koppe, P. Denk, C. Waldauf, A. J. Heeger, C. J. Brabec, *Adv. Mater.* **2006**, *18*, 789.